Monitoring Fracture Healing Using Digital Radiographies

Gang Li and Mark Murnaghan

The Department of Orthopaedic Surgery, Queen's University Belfast, Musgrave Park
Hospital, Stockman's Lane, Belfast, BT9 7JB, UK
e-mail:g.li@qub.ac.uk

Abstract

Non-invasive imaging of fracture healing is a crucial step in making clinical decisions for optimal outcomes and minimizing risks of fixator removal. Although orthogonal routine radiography remains the most cost effective imaging technique to follow all aspects of fracture healing, it is not reliable to predict bony union or the quality or quantity of the regenerating bone, since an estimated 40% increase in radiodensity is needed to visualize a radiological change, and radiographic changes do not always correlate to mechanical stiffness. Supplemental techniques, including digital radiography, mechanical testing for bone strength and stiffness, dual-energy X-ray absorptiometry (DXA) for bone mineral density (BMD), quantitative computed tomography (QCT) for density and cortical continuity, ultrasound for cyst detection and Doppler or angiography for assessing local blood flow and vascularity, have all been used clinically. Among the methods, digital radiography is a useful, cost-effective and relatively accurate means in the evaluation of new bone formation with time during fracture healing. In animal models of fracture healing, histological data, not the mechanical stiffness of the fracture, showed a positive correlation with the digital radiographic assessment data (relative bone density). The advantages of using digital radiography are the minimal expense and dynamic observation of the healing process through sequential radiographies. The bone-healing qualities can be assessed through the estimated relative bone (mineral) density using phantoms. There is a burning need for a quantitative measure of fracture healing in long bone fractures treated by intramedullary nailing. As there is no prospect of a mechanical measure due to the load-sharing design of the fracture/nail construct, radiological imaging has to be the starting point. After normalization, calibration and registration of serial images, a combination of functional images are be used to monitor the changing mineral content of the tissues in and around the fracture; however, due to its 2D nature, the digital radiographies need to be taken in a standard fashion to allow sequential comparison, and it should be used as a complementary, rather than an absolute, measurement for fracture healing.

Fracture Healing Animal Model

A fracture model is a system employed to study fracture healing, which is of relevance to human fracture healing as encountered in medical practice. The most representative (valid) model would therefore be a human fracture; however, the high validity of a human fracture model must be balanced against poor reliability due to extensive variation between cases in clinical practice. At the opposite extreme, cell culture models are much more reliable but are deficient in validity as a representation of the whole fracture-healing process. Between these extremes lie models in various species and sizes of animal, which offer the possibility of adequate numbers of reasonably similar cases of fracture healing occurring in a whole-organism context, in other words, a balance between reliability and validity.

Model reproducibility is essential for valid investigation and comparison of fracture healing. Several small and large animal models are reported for the investigation of fracture repair in mice (Bunn et al. 2004; Connolly et al. 2003; Li et al. 2005), rats (Bonnarens and Einhorn 1984; Greiff 1978; Olmedo 1994), rabbits (Critchlow 1995), sheep (Claes et al. 1998), dogs (Wu et al. 1984) and goats (Welch et al. 1998). All investigations included variation of important influences on bone repair such as the nature of the fracture, its stability, mechanical stress environment, the fixation device applied and success of fracture reduction. Small animals, such as the mouse, are attractive candidates for investigating bone healing, particularly for studies focused on molecular questions, because of the availability of gene knockouts, antibodies and gene probes (Metsaranta et al. 1991). An externally fixated murine femoral osteotomy model has been developed, validated and used to study various aspects of fracture healing (Bunn et al. 2004; Connolly et al. 2003; Li et al. 2005; Murnaghan et al. 2005).

Monitor Digital Radiographies in Animal Model of Fracture Healing

Standardization of Taking Digital Radiographies

In order to obtain standardized digital radiography, a standardized protocol has to be set up for each study. For instance, we used Faxitron MX-20 digital radiography system for the purposes of taking all X-rays of our animal studies (Fig. 1). Before a day surgery was begun, the machine was turned on and calibrated by taking a series of

Figure 1. Faxitron M20 digital radiography system

Figure 2 a,b. a X-ray jig for mouse fracture model. **b** Mouse with external fixator and the X-ray jig immediately before digital radiography being taken
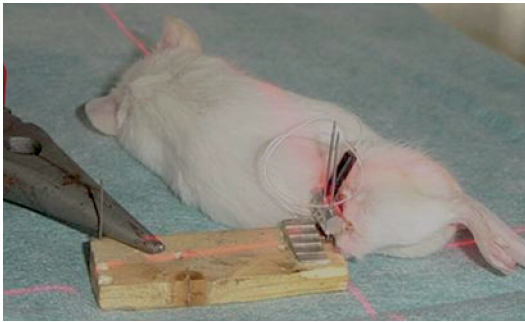
Figure 3. Standardization of the X-ray position. The phantom and jig is held flat to the plate using an overlying weight and a crosshair laser is used to centre the area of interest such that a repeatable film may be obtained and comparisons between subsequent pictures is possible

eight X-rays (26 kV, 10 ms) to ensure normalization of exposure of radiation. At the end of the surgical procedure (or following induction of a light general anaesthesia for X-rays taken from day 4 onwards), an X-ray jig (Fig. 2) was attached to the cross bar through the two perpendicular portals. This jig contained an aluminium step phantom and allowed for normalization of X-ray penetration between animals and across time points. It also controlled for rotation in all planes, therefore enabling comparison of changes at the fracture within animals.

For taking the X-ray, the animal is carefully placed prone inside the X-ray compartment with its left leg held flexed and in external rotation such that a lateral radiograph of the femur can be taken. The phantom and jig are held flat to the plate using an overlying weight and a crosshair laser is used to centre the area of interest such that a repeatable film may be obtained and comparisons between subsequent pictures can be possible (Fig. 3). The distance from the beam to the plate remains the same throughout the experiment (e.g. 12 cm), and X-rays are taken using a fixed set of exposure setting, such as 24 KPa for 3 s for the mouse. Digital X-rays are then saved in the source computer in the operating theatre as raw data files (*.dat).

Analysing Digital Radiographies

The raw data files of the digital radiographies are subsequently analysed using the freely available image analysis software from the University of Texas Health Science Centre San Antonio Dental School (http://ddsdx.uthscsa.edu/). Following several pilot studies into methods of analysis of the data, two standardized techniques are employed for analysing all X-rays. Both methods use the assumption that increasing bone density equates to an increase in pixel density on the radiographs. In each method the bone density at the fracture gap is measured and changes at the site compared across time points and also across drug groups.

The first method is referred to as the "line method". Three parallel lines, 75 pixels in length and centred on the fracture gap, are drawn parallel to the axis of the femoral shaft (Fig. 4). A mean value for each of the 75 points along the femur is calculated
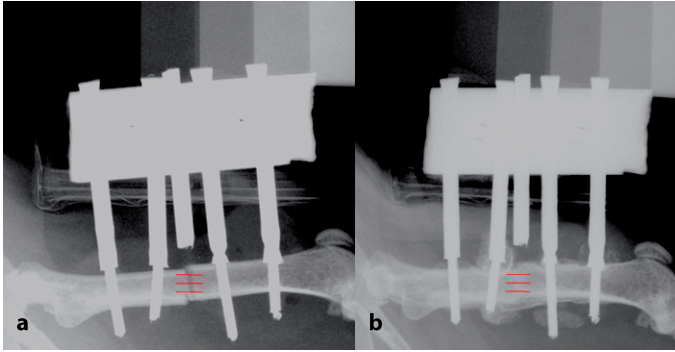
Figure 4a,b. Mouse femoral fracture digital X-rays shows lines for density analysis at day 0 (**a**) and day 32 (**b**) following fracture

from the three lines (Fig. 5a,b). The variances in pixel density of the femur as you pass proximally to distally can then be assessed and plotted as a line graph of pixel density against distance. The 75-pixel length is then divided into three equal 25-pixel sections comprising areas of "normal" bone adjacent to the fracture both proximally and distally alongside a 25-pixel length comprising the fracture gap itself (Fig. 5c). The mean pixel density of the adjacent areas of bone is calculated (solid line) and the
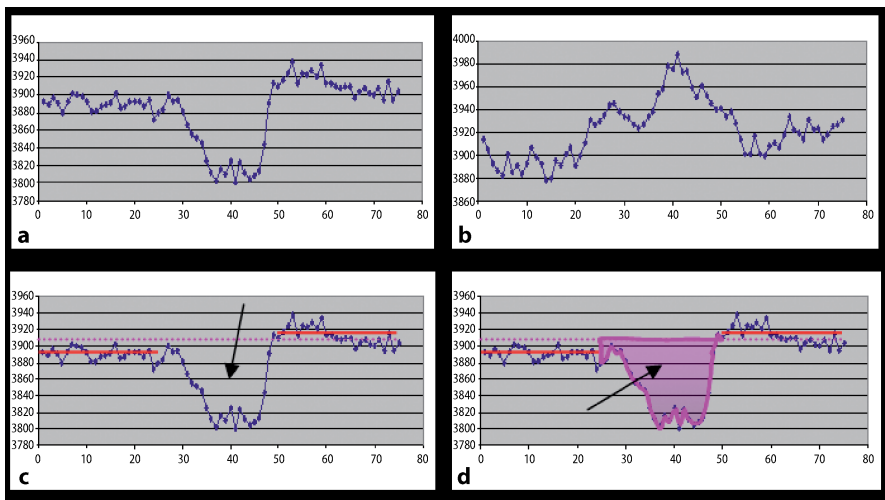
Figure 5a–d. Line plots of density measurement from a raw data file of digital radiography at day 0 of fracture (**a**) and at day 32 post-fracture (**b**). **c** The 75-pixel length is then divided into three equal 25-pixel sections comprising the areas of "normal" bone adjacent to the fracture both proximally and distally alongside a 25-pixel length comprising the fracture gap itself (*arrow*). **d** The mean pixel density of the adjacent areas of bone is calculated (*solid line*) and the difference to this mean (*dotted line*) for the central section comprising the fracture gap is then calculated from the area under the curve (*shaded area, arrow*)
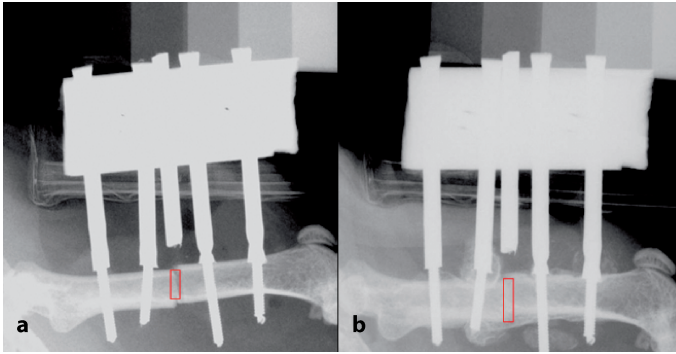
Figure 6 a,b. Density assessment is referred to as the "area method". **a** *Boxed area* represents fracture gap at day 0 of fracture. **b** The *boxed area* represents fracture gap at day 32 following fracture

difference to this mean (dotted line) for the central section comprising the fracture gap is then calculated from the AUC (shaded area) in Fig. 5d. A comparison can be made as to how the bone content at the fracture gap changes over time. Initially, there is relatively less bone content at the fracture gap, but this becomes positive as callus is laid down during the repair process.

The second method of density assessment is referred to as the "area method" and is performed by measuring the mean pixel density of bone at the fracture gap itself (Fig. 6). Using the image analysis software the mean pixel density of a standardized rectangle centred over the fracture gap approximately 0.5 mm in diameter and extending to the inner edge of the cortices is measured. Alterations in bone density due to variances in X-ray exposure are accounted for by standardization to the aluminium phantom attached to the X-ray jig. The line method also utilizes an internal method of standardization as changes in density are presented as a ratio to the normal femur such that any changes in X-ray exposure will affect both the fracture gap and adjacent normal bone equally.

Reliability of the Digital Radiography Measurement

The intra-observer correlation analysis for the digital radiographic analysis has suggested that the mechanisms of deriving data values and the subsequent analysis of those values are highly repeatable with very low levels of intra-observer errors being observed. By using two independently derived variables across each of the outcome measures [digital X-ray, AUC and region of interest (ROI)]; biomechanical testing, peak loads and stiffness), we have been able to correlate the results both within each outcome measure (i.e. peak load with stiffness; AUC with ROI; Fig. 7a) and across outcome measures (i.e. AUC with histology, AUC with rigidity, etc.; Fig. 7b,c). It has demonstrated that these outcomes correlate very well with strong positive correlations seen both within each of the outcomes (illustrated are ROI with AUC; Fig. 7a); however, there are no significant associations between the day-24 X-ray and biome-

a
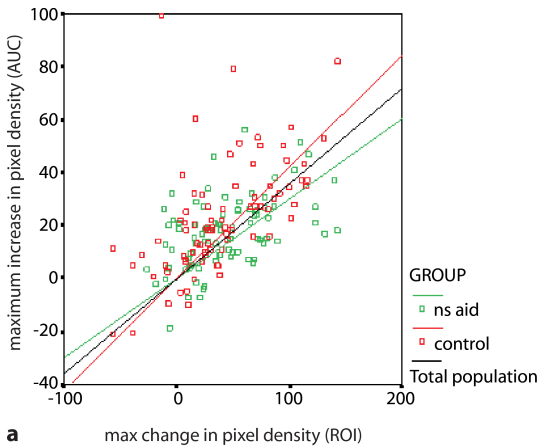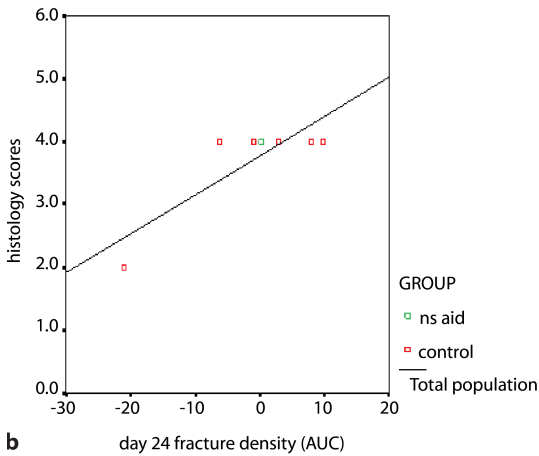
b
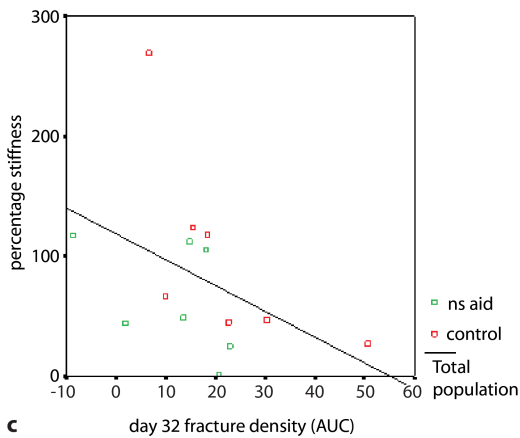
c

Figure 7 a–c. a Comparisons made between the two methods of radiological assessments, i.e. the area under the curve (AUC) and region of interest (ROI) modalities. To assess this, the maximum change in pixel density from day 0 for each modality is used. Scatter plot of data from AUC and ROI analysis shows a strong correlation between the two methods. **b** At day 32, there is a significant correlation noted between the histology scores and relative fracture density measured from the digital radiographies (Spearman's correlation; $R = 0.626$; $p = 0.013$). **c** Correlations across radiological and biomechanical data produced few statistically significant results. There are no significant associations between the day-24 X-ray and biomechanical data. At day 32, however, there is a strong negative association between the AUC X-ray data and the stiffness of the femurs (Spearman test: $R = -0.687$; $p = 0.010$)
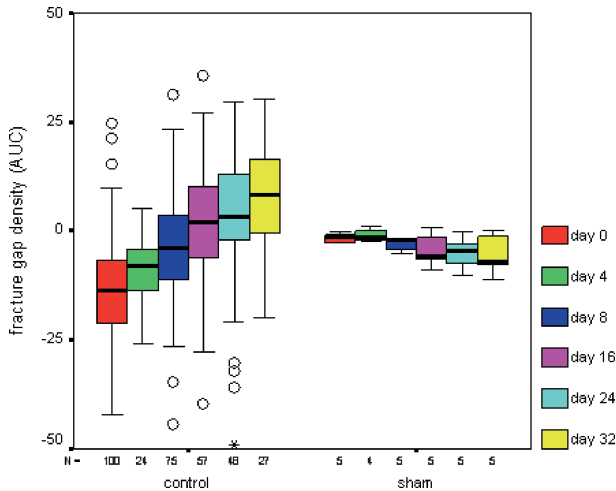
Figure 8. Digital radiography analysis shows changes in the fracture gap density in the two groups (control is the fracture group and sham is the group with fixator but no fracture). The measurement is sensitive enough to identify the more subtle decrease in the sham-group density profile. In the fracture group, the density of the fracture gap at day 16 reaches its peak

chanical data. At day 32, however, interestingly there is a strong negative association between the AUC X-ray data and the stiffness of the femurs (Spearman test: $R = -0.687$; $p = 0.010$). The validity of the radiological outcomes used in demonstrating real changes across the fracture gap density between the control and experimental fracture animals (Fig. 8). The technique is capable of differentiating between the changes in the fracture gap density between the two groups of animals, it is also sensitive enough to identify the more subtle decrease in the sham-group density profile (Fig. 8).

Clinical Considerations of Digital Radiography Analysis

Clinical Needs

Orthopaedic surgery has great need of objective and quantitative measures of fracture healing, especially in the reputedly unsolved tibial shaft fracture (Aronson and Shin 2003). In intramedullary nailed fractures stiffness measurements are not possible, which leaves radiological assessment as the only realistic way to monitor the progress of healing. Our pilot study has evaluated the bone mineral density (BMD) of test samples by using digital X-ray images which have been calibrated with a hydroxyapatite reference phantom. Our results compare favourably to results on the same test samples evaluated by DXA, the current gold standard of BMD evaluation. We have also performed preliminary analysis of serial images of nailed tibial fractures that have progressed to union (Fig. 9). The use of imaging phantoms is a common method of evaluating image quality in the clinical setting. These evaluations rely on a subjective decision by a human observer with respect to the faintest detectable signal(s) in the image. Because of the variable and subjective nature of the human-observer scores, the evaluations manifest a lack of precision and a potential for bias.
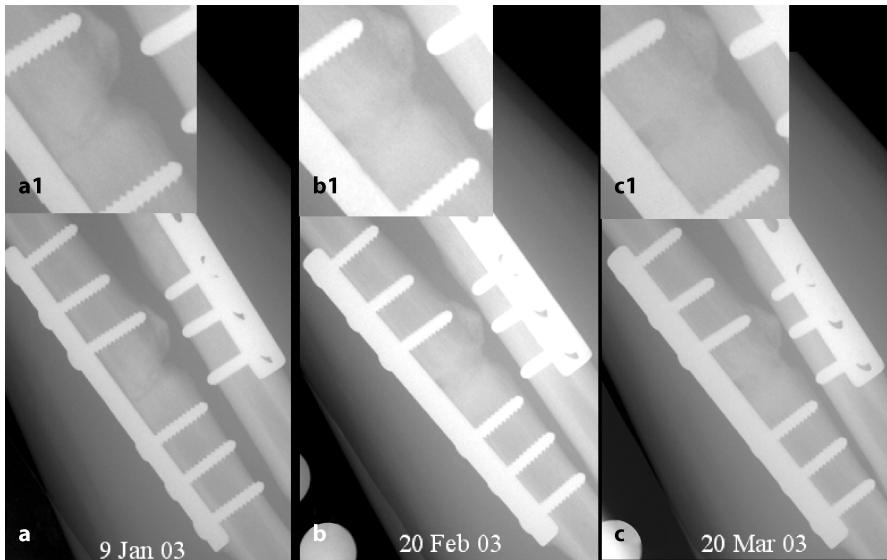
Figure 9 a–c. Serial digital radiographies obtained from a tibial fracture patient with standard-ised X-ray jig over a 3-month period (**a-c**), showing the progress of fracture healing. *A1 − C1* close-ups of the fracture gap in **a-c**

The advantage of digital imaging systems with their inherent digital data provides the opportunity to use techniques that do not rely on human-observer decisions and thresholds (Gagne et al. 2003, 2006).

Considerations for Clinical Applications

In clinical practice, before the serial digital radiographies can be used for comparison purposes, the digital images have to be calibrated, normalized and registered. Image registration may be achieved firstly by standardizing the geometry during acquisition of the image using a position control device (Fig. 10), and subsequently by using computer algorithms to match the images to subpixel accuracy. There are still some technical challenges ahead, such as scatter removal via deconvolution and soft tissue removal with beam-hardening correction. Deconvolution is the mathematical process that allows reconstruction of the desired image from the actual radiograph. Once the registration of the image series is completed, the resultant serial images are analysed using functional imaging, morphological description, and 3D reconstruction from two orthogonal views. There is ongoing work in this filed to perfect and standardize the techniques before they can be applied reliably (Gagne et al. 2003; Hazelwood and Burton 2006; Siewerdsen et al. 2006). Nevertheless, animal work has proved that digital radiography can be used as a tool for monitoring fracture healing. Due to the 2D nature of radiography, digital radiographies need to be taken in a standard fashion to allow meaningful sequential comparison, and the facilities for digital

Figure 10. X-ray jig (*solid arrow*) is applied to control the standard position of the limb for taking X-ray, and settings on the jig (for the limb position and angles) are recorded for each patient and used at subsequent visits. Hydroxyapatite phantoms (*shaded arrow*) are placed on the digital X-ray cassette for measuring relative density

radiography follow-up of human fracture healing must be developed with an experienced radiologist, and it is only recommended where this possibility exists. Finally, in animal models of fracture healing, histological data, not the mechanical stiffness of the fracture, show a positive correlation with the digital radiographic assessment data (relative bone density), suggesting that the radiographies shall always be used as a complementary tool in conjunction with clinical and other means of assessment of fracture healing.

Conclusion

Digital radiography is a useful, cost-effective and relatively accurate means of evaluating and following new bone formation during fracture healing. It allows continuous assessment of the healing process through sequential radiographies. In animal models of fracture healing, histological data, but not the mechanical stiffness of the fracture, showed a positive correlation with the digital radiographic assessment data such as relative bone density. The bone-healing qualities can be assessed through the estimated relative bone (mineral) density using phantoms; however, due to its 2D nature, the digital radiographies need to be taken in a standard fashion to allow sequential comparison, and it should be used as a complementary? rather than an absolute?measurement for fracture healing.

References

Aronson J, Shin HD (2003) Imaging techniques for bone regeneration analysis during distraction osteogenesis. J Pediatr Orthop 23:550–560

Bonnarens F, Einhorn TA (1984) Production of a standard closed fracture in laboratory animal bone. J Orthop Res 2:97–101

Bunn JR, Canning J, Burke G, Mushipe M, Marsh DR, Li G (2004) Production of consistent crush lesions in murine quadriceps muscle: a biomechanical, histomorphological and immunohistochemical study. J Orthop Res 22:1336–1344

Claes LE, Heigele CA, Neidlinger-Wilke C, Kaspar D, Seidl W, Margevicius KJ, Augat P (1998) Effects of mechanical factors on the fracture healing process. Clin Orthop Relat Res 355 (Suppl): S132-S147

Connolly CK, Li G, Bunn JR, Mushipe M, Dickson GR, Marsh DR (2003) A reliable externally fixated murine femoral fracture model that accounts for variation in movement between animals. J Orthop Res 21:843–849

Critchlow MA, Bland YS, Ashhurst DE (1995) The effect of exogenous transforming growth factor-beta 2 on healing fractures in the rabbit. Bone 16:521–527

Gagne RM, Boswell JS, Myers KJ (2003) Signal detectability in digital radiography: spatial domain figures of merit. Med Phys 30:2180–2193

Gagne RM, Gallas BD, Myers KJ (2006) Toward objective and quantitative evaluation of imaging systems using images of phantoms. Med Phys 33:83–95

Greiff J (1978) A method for the production of an undisplaced reproducible tibial fracture in the rat. Injury 9:278–281

Hazelwood S, Burton D (2006) Images in clinical medicine. N Engl J Med 354:e6

Li G, Bunn JR, Mushipe MT, He Q, Chen X (2005) Effects of pleiotrophin (PTN) over-expression on mouse long bone development, fracture healing and bone repair. Calcif Tissue Int 76:299–306

Metsaranta M, Toman D, De Crombrugghe B, Vuorio E (1991) Specific hybridization probes for mouse type I, II, III and IX collagen mRNAs. Biochim Biophys Acta 1089:241–243

Murnaghan M, McIlmurray L, Mushipe MT, Li G (2005) Time for treating bone fracture using rhBMP-2: a randomised placebo controlled mouse fracture trial. J Orthop Res 23:625–631

Olmedo ML, Weiss AP (1994) An experimental rat model allowing controlled delivery of substances to evaluate fracture healing. J Orthop Trauma 8:490–493

Siewerdsen JH, Daly MJ, Bakhtiar B, Moseley DJ, Richard S, Keller H, Jaffray DA (2006) A simple, direct method for X-ray scatter estimation and correction in digital radiography and cone-beam CT. Med Phys 33:187–197

Welch RD, Jones AL, Bucholz RW, Reinert CM, Tjia JS, Pierce WA, Wozney JM, Li XJ (1998) Effect of recombinant human bone morphogenetic protein-2 on fracture healing in a goat tibial fracture model. J Bone Miner Res13:1483–1490

Wu JJ, Shyr HS, Chao EY, Kelly PJ (1984) Comparison of osteotomy healing under external fixation devices with different stiffness characteristics. J Bone Joint Surg Am 66:1258–1264